GDCh

Research Articles

Angewandte
Chemie
International Edition
www.angewandte.org

A Three-Dimensional Inorganic Analogue of 9,10-Diazido-9,10-Diboraanthracene: A Lewis Superacidic Azido Borane with Reactivity and Stability

Chonghe Zhang, Xiaocui Liu, Junyi Wang, and Qing Ye*

Abstract: Herein, we report the facile synthesis of a three-dimensional (3D) inorganic analogue of 9,10-diazido-9,10-dihydrodiboraanthracene, which turned out to be a monomer in both the solid and solution state, and thermally stable up to 230 °C, representing a rare example of azido borane with boosted Lewis acidity and stability in one. Apart from the classical acid-base and Staudinger reactions, E–H bond activation (E = B, Si, Ge) was investigated. While the reaction with B–H (9-borabicyclo[3.3.1]nonane) led directly to the 1,1-addition on N_α upon N_2 elimination, the Si–H (Et$_3$SiH, PhMe$_2$SiH) activation proceeded stepwise via 1,2-addition, with the key intermediates 5_{int} and 6_{int} being isolated and characterized. In contrast, the cooperative Ge–H was reversible and stayed at the 1,2-addition step.

Introduction

How to find an optimal balance between reactivity and stability is a recurring theme in molecular design, particularly those related to reaction chemistry. Azido boranes

[*] C. Zhang, X. Liu, J. Wang, Q. Ye
    Department of Chemistry,
    Southern University of Science and Technology
    518055 Shenzhen (P. R. China)
    E-mail: qing.ye168@gmail.com

    J. Wang
    Department of Chemistry,
    The Hong Kong University of Science and Technology
    Clear Water Bay, Kowloon, Hong Kong (Hong Kong)

    Q. Ye
    Institute for Inorganic Chemistry,
    Julius-Maximilians-Universität Würzburg,
    Am Hubland, 97074 Würzburg (Germany)
    and
    Institute for Sustainable Chemistry & Catalysis with Boron,
    Julius-Maximilians-Universität Würzburg
    Am Hubland, 97074 Würzburg (Germany)
    E-mail: qing.ye@uni-wuerzburg.de

with the general formula of $R_{(3-n)}B–(N_3)_n$ ($n = 1–3$) are well recognized for their applications in energetic materials and as synthetic intermediates.[1] The reported reactivity patterns of azido boranes are mostly azido-based, including the [3+2]-dipolar cycloaddition reactions,[1b–d] Staudinger reactions,[1v] 1,1-addition,[1a] and R-group migration reactions that are associated with N_2 elimination.[1e–h] There are notably less reactions of azido boranes in which boron is a non-spectator, perhaps because the azido boranes of enough stability usually require electronic stabilization either by quaternization with a σ-donating ligand[1b,c,h,i,l,2] or by substitution with π-donating groups,[1a,d,j,k,m] which nevertheless turns off the reactivity at boron. The azido boranes with boosted Lewis acidity but lacking steric hindrance tend to aggregate via intermolecular B–N interaction.[1n–u] For instance, the dihaloazidoboranes $(BX_2N_3)_3$ (X = F, Cl, Br) with small and electron-withdrawing halogens exist as trimers.[1o,s–u] $(F_5C_6)_2BN_3$ and $(2,6-F_2C_6H_3)_2BN_3$ bearing two electron-withdrawing fluorinated aryl groups exist as monomer in solution, but dimerize in the solid state (Figure 1).[1p–r] The strongly Lewis acidic 9-azido-9-borafluorene, which features an azidoborole unit, was first synthesized by the Bettinger group. Likewise, the 9-azido-9-borafluorene was synthesized as a monomer in solution but transformed into a cyclotrimer when solvent was removed.[1n] The monomeric 9-azido-9-borafluorene is highly reactive perhaps due to the coexistence of a strongly Lewis acidic boron and an adjacent Lewis basic nitrogen center. The N_2 elimination of 9-azido-9-borafluorene could be thermally induced, affording a BN-phenanthryne intermediate, which can undergo cyclotrimerization to give a structurally characterized tetramer, or be trapped with trimethylchlorosilane or the second equivalent of 9-azido-9-borafluorene.[1g] Considerable efforts towards the combination of an azido group and a non-fused borole moiety in one molecule can be seen in a very recent report by Braunschweig and co-workers.[2] However, the 1-azido-2,3,4,5-tetraphenylborole turned out to be even less stable than 9-azido-9-borafluorene and had to be trapped at −75 °C with a Lewis base as evidence for its formation.[2] Thus overall, the knowledge about the reactivity of strongly Lewis acidic azido boranes is still limited. The dearth of related research is presumably attributed to the pronounced instability, capricious nature or poor solubility caused by aggregation.

9,10-Dihydro-9,10-diboraanthracenes (DBAs) are boron congeners of anthracenes in which the sp^2-hybridized carbons at 9- and 10-positions are replaced by a trigonal
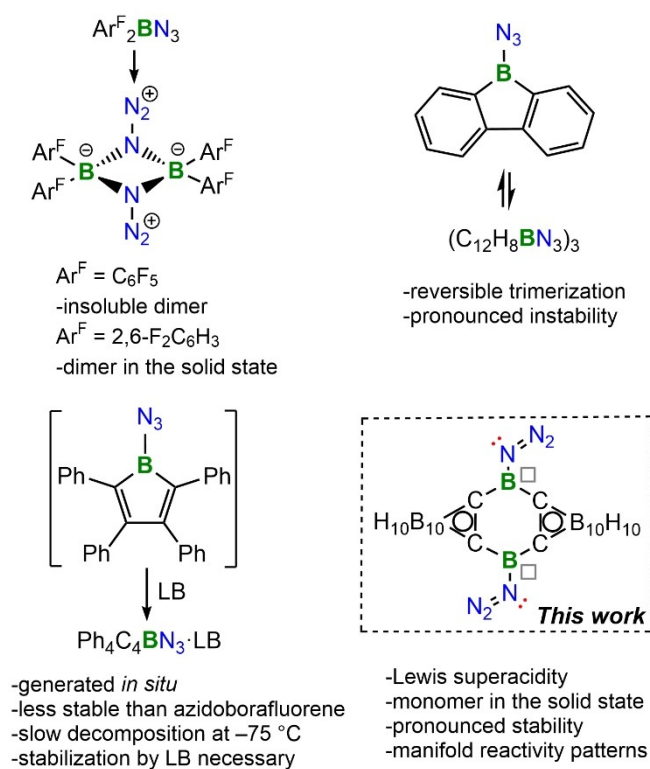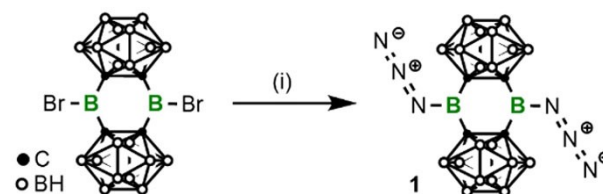
Figure 1. Representative examples of strongly Lewis acidic azido boranes and the robust Lewis superacidic azido borane in this work. "□" represents the empty p_z-orbital of boron, ":" represents the electron lone pair of N_α.

Results and Discussion

The azido borane $(C_2B_{10}H_{10})_2(BN_3)_2$ (**1**) was attained by the reaction of $(C_2B_{10}H_{10})_2(BX)_2$ (X = Cl, Br) with 2.3 equivalents of TMSN$_3$ (Scheme 1). The bridging boron atoms displayed broad singlet signals at δ_B 41.8 in the ^{11}B-NMR spectrum. After easy work up, **1** could be isolated as a white powder in excellent yield (97%). Single crystal X-ray diffraction analysis unambiguously confirmed the monomeric structure of compound **1** (Figure 3) in the solid state. The B1–N1 bond (1.407(2) Å) is lightly shorter than that of the tricoordinate azido boranes stabilized by π-donating groups (1.433 Å to 1.468(4) Å),[1j,k,m] which could be attributed to the more acidic boron center of **1**. The nearly mutual orthogonal orientation between the vacant p-orbital on boron and the electron lone pair on N_α (∠N2–N1–B1–C1 4.50°) prevents the direct N→B π-interaction. The geometric parameters of the azido group fall in the expected range. IR spectrum displayed strong absorption band at 2159 cm^{-1} for the azido groups (Figure S35). The assignment of the IR absorption was confirmed by the calculated harmonic vibrational frequencies (Table S1).

The strength of Lewis acidity of **1** was studied by Gutmann-Beckett method. The ^{31}P Δδ value of 37.83 in C_6D_6 suggested a greater Lewis acidity of **1** than that of $B(C_6F_5)_3$ (^{31}P Δδ 29.66 in C_6D_6).[13] The fluoride ion affinity (FIA) of **1** was calculated according to the protocol proposed by Krossing.[14] The value of 9.6 kcal mol^{-1} is higher than that of

planar boron center, respectively, leading to a neutral conjugated π-system but with two fewer π electrons than anthracene. DBAs, their doubly reduced derivatives (DBA)$^{2-}$ as well as the N-heterocyclic carbene (NHC) stabilized derivatives demonstrated unique photophysical properties and diverse reactivity, allowing for the applications in ligand design,[3] olefin polymerization,[4] luminescent materials,[5] dihydrogen- and hydride-transfer catalysis,[6] small molecule activation,[6,7] and fluoride complexation.[8] Inspired by the fascinating features of DBAs and following the two-dimensional/ three-dimensional (2D/3D) relationship between benzyne and carboryne,[9] we designed and successfully synthesized the first 3D analogues of DBA, in which the benzyne units are replaced by *o*-carboryne groups.[10] Indeed, our experimental and computational results revealed the Lewis superacidity at the bridging trigonal planar boron centers, which should be induced by the strong electron withdrawing effect of the *o*-carborane cage[11] and its minimized π-interaction with the vacant p-orbital of boron. Given the paucity of 2D 9,10-diazido-DBA, which is of considerable synthetic challenge, we herein set out to synthesize and investigate its first 3D inorganic analogue. Benefitting from the electronic and kinetic stabilizing effect of the carborane cage,[12] the 3D 9,10-diazido-DBA represented a rare example of azido borane of boosted Lewis acidity whilst stable—an optimal platform for reactivity investigation.

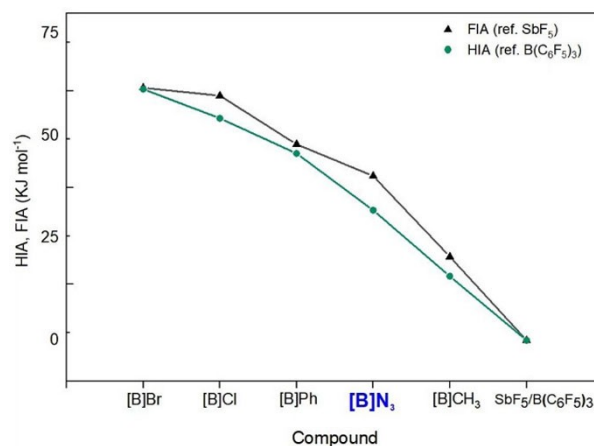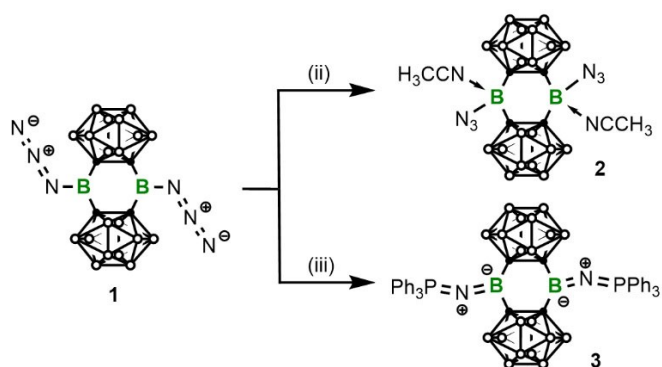**Scheme 1.** Synthesis of **1**. (i) 2.3 equivalents of TMSN$_3$, room temperature, 30 mins.

Figure 2. FIA (referenced to SbF$_5$), and HIA (referenced to $B(C_6F_5)_3$) of compound **1** and the other 3D analogues of DBA in sequence.

Scheme 2. Synthesis of **2** and **3**. (ii) excess acetonitrile in toluene, room temperature, 1 day; (iii) 2.0 equivalents of PPh₃ in toluene, room temperature, 30 mins.
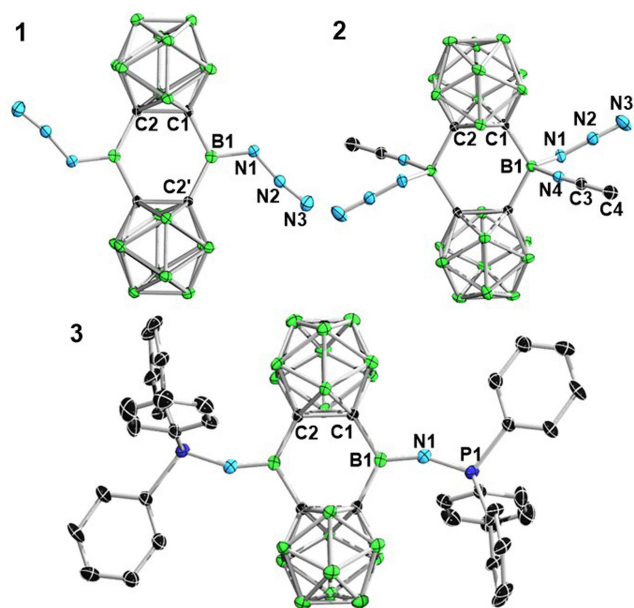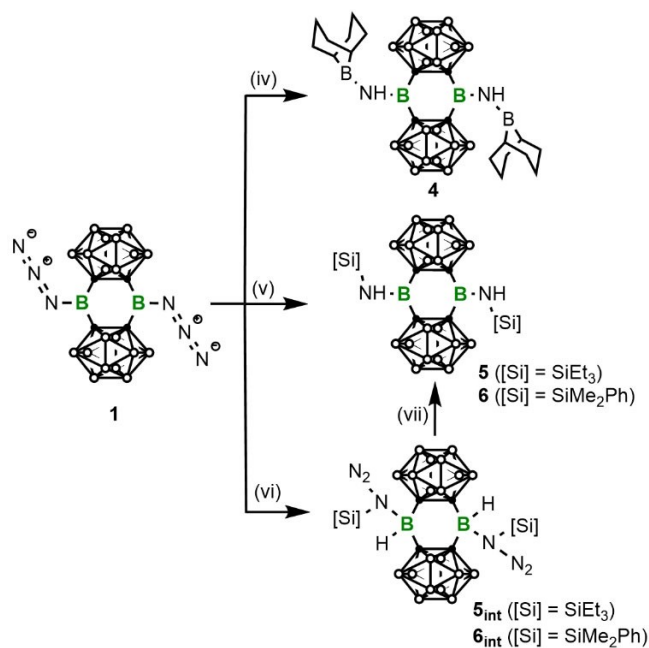

Figure 3. Single crystal structures of **1–3**. Hydrogen atoms and co-crystalized toluene molecule in **3** have been omitted for clarity. Thermal ellipsoids are drawn at 50% probability level for **1** and **3**, and 30% probability level for **2**. Selected bond lengths [Å] and angles [°]: for **1**, B1–N1 1.407(2), C1–B1 1.587(2), N1–N2 1.254(2), N2–N3 1.125(2), C1–C2 1.667, C2'–B1–C1 122.66(13), C1–B1–N1 112.31(13), C2'–B1–N1 124.99(13), B1–N1–N2 126.29(13), N1–N2–N3 170.28 (15), C1–B1–N1–N2 −175.50; for **2**, B1–C1 1.650(5), B1–N1 1.537(4), N1–N2 1.234(3), N2–N3 1.149(3), B1–N4 1.605(4), N4–C3 1.150(3), C3–C4 1.450(4), B1–N1–N2 121.87(29), N1–N2–N3 174.3(2), B1–N4–C3 172.7(2); for **3**, B1–C1 1.597(4), B1–N1 1.352(4), N1–P1 1.562(2), B1–N1–P1 156.9(2).

Scheme 3. Synthesis of **4–6** and intermediates **5int** and **6int**. (iv) 1.1 equivalents of 9-BBN dimer in toluene, 60 °C, 1 day; (v) for **5**, 2.3 equivalents of Et₃SiH, 60 °C in toluene, 30 mins; for **6**, 2.3 equivalents of PhMe₂SiH, 60 °C in toluene, 1 day; (vi) for **5int**, excess Et₃SiH, −30 °C in CH₂Cl₂, 5 days; for **6int**, excess PhMe₂SiH, −30 °C in toluene, 5 days; (vii) for **5**, 3 days at 38 °C in the solid state, 30 min at 60 °C in toluene; for **6**, 1 day at 60 °C in toluene.
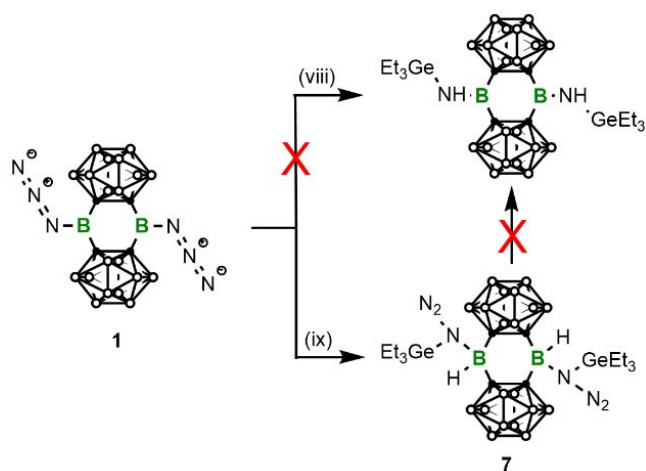
Scheme 4. Synthesis of **7**. (viii) 4 equivalents of Et₃GeH in C₆D₆, 60 °C, 30 mins; (ix) 4 equivalents of Et₃GeH in toluene, −30 °C, 5 days.

SbF₅, thus confirming its Lewis superacidity.[15] The soft nature of the bridging boron centers was verified by the calculated hydride ion affinity (HIA) that is 7.6 kcal mol⁻¹ higher than that of B(C₆F₅)₃. Overall, the Lewis acidity of the azido borane **1** should fall between the phenyl and methyl derivatives by comparison of their FIA and HIA values (Figure 2). Furthermore, the calculated LUMO is mostly located on the bridging boron centers, while the

HOMO indicates weak nucleophilicity of Nα atom (Figure S59). Gratifyingly, compound **1** displayed remarkable thermal and photo stability. The differential scanning calorimeter (DSC) experiments suggested a thermal stability up to 230 °C (Figure S49). The irradiation of **1** by a Xenon lamp for 3 days did not lead to any obvious decomposition either.

The Lewis base adduct **2** (Scheme 2) was obtained as a crystalline solid by adding excess acetonitrile (ACN) into
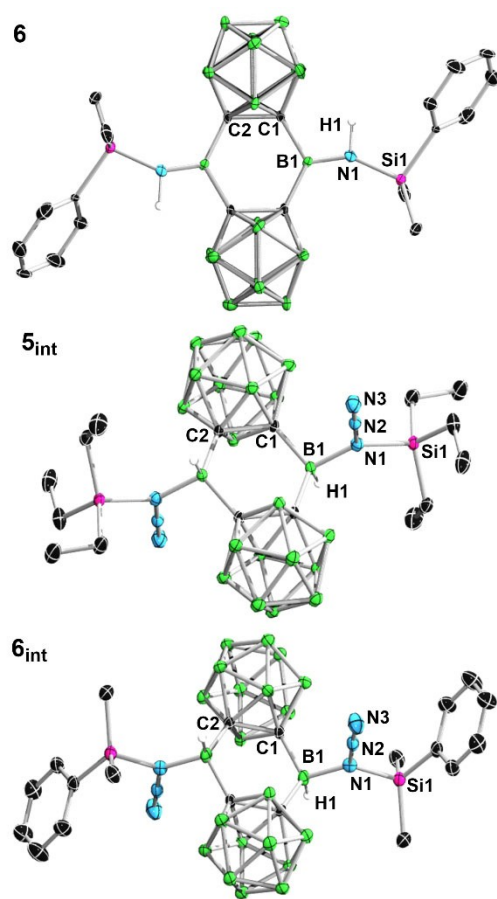
Figure 4. Single crystal structure of **6**, **5**$_{int}$ and **6**$_{int}$. Hydrogen atoms, except for those bound to a 4-coordinate boron or a secondary amino group, have been omitted for clarity. Thermal ellipsoids are drawn at 50% probability level. Selected bond lengths [Å] and angles [°]: for **6**, B1–C1 1.607(5), C1–C2 1.675, B1–N1 1.382(5), N1–Si1 1.783(3), N1–H1 0.84(4), B1–N1–Si1 150.1(3), B1–N1–H1 107(3), H1–N1–Si1 103(3); for **5**$_{int}$, B1–H1 1.00, B1–N1 1.626(2), B1–Si1 3.118, N1–Si1 1.856(1), Si1–H1 3.072, N1–N2 1.268(2), N2–N3 1.122(2), H1–B1–N1 106.5, B1–N1–Si1 126.92(9), Si1–N1–N2 115.13(10), B1–N1–N2 117.93(12), N1–N2–N3 179.50(16); for **6**$_{int}$, B1–C1 1.643(4), C1–C2 1.699(4), B1–H1 1.00, B1–N1 1.623(4), N1–Si1 1.858(3), N1–N2 1.267(4), N2–N3 1.127(4), Si1–H1 3.039, B1–N1–Si1 125.4(2), N1–N2–N3 179.2 (3).

Figure 5. The Et$_3$SiH adducts of **LA**$_{1–3}$ and **5**$_{int}$ and their corresponding Si–H bond lengths.

the toluene solution of **1**. The single crystal structure (Figure 3) revealed two tetracoordinate boron centers, and thus confirming the reaction stoichiometry (**1**+2 ACN). The IR spectrum of **2** displayed absorption at 2353 cm^{-1} for the coordinated ACN (Figure S36), being ca. 87 cm^{-1} red shifted with respect to the free ACN, which is attributed to the Lewis superacidity of **1**.[16] The addition of PPh$_3$ into a toluene solution of **1** did not lead to the corresponding Lewis base adduct, but triggered N$_2$ elimination instead, giving the Staudinger reaction product **3** as a crystalline solid (Figure 3).[1v,17] The B–N (1.352(4) Å) and N–P (1.562(2) Å) distances of **3** are comparable to those in (C$_6$F$_5$)$_2$B–N=P^{t}Bu$_3$ (B<C->N 1.344(4) Å, N<C->P 1.560(3) Å).[1v]

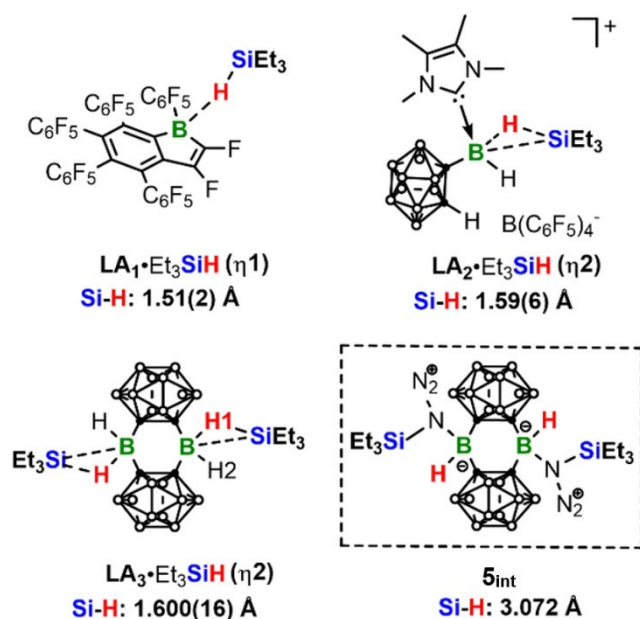The reaction of **1** with 2 equivalents of 9-borabicyclo-[3.3.1]nonane (9-BBN) in toluene was performed at 60°C,

and monitored by multinuclear NMR spectroscopy (Scheme 3). The ^{11}B-NMR spectra revealed gradual conversion of **1** (δ_B 41.8) and 9-BBN (δ_B 27.9) into **4** (δ_B 38.3, 65.0). It should be noted that neither the ^{11}B- nor the ^{1}H-NMR spectra indicated any intermediate. Likewise, the reactions of **1** with 2 equivalents of tertiary silanes at 60°C afforded **5** (δ_B 37.9) and **6** (δ_B 39.0). Thus, compounds **4–6** all appear to be the products of N$_2$-elimination and 1,1-addition of E–H (E=B, Si) bond on nitrogen. The atom connectivity of **6** could be confirmed by single crystal X-ray diffraction analysis (Figure 4). The B1–N1 (1.382(5) Å) distance in **6** is somewhat shorter than that (1.407(2) Å) in **1** with weak B–N π interaction (see above), and notably shorter than that (1.537(4) Å) in **2**, in which the B–N π interaction is precluded.

It should be noted that the intermediates **5**$_{int}$ (δ_H 0.64, SiCH$_2$CH$_3$) and **6**$_{int}$ (δ_H 0.34, SiCH$_3$) during the formation of **5** and **6** were clearly observed on the reaction monitoring NMR spectra. In order to isolate and characterize the intermediates, the reactions were carried out at low temperatures. Storage of a dichloromethane (DCM) solution of **1** and a large excess of HSiEt$_3$ or HSiMe$_2$Ph at −30°C for 5 days afforded **5**$_{int}$ or **6**$_{int}$ as a crystalline solid, respectively. In stark contrast to the previously reported borane-silane adducts **LA$_1$**·Et$_3$SiH (Figure 5),[18] which displayed a broad signal at δ_B 36.8 at room temperature, compounds **5**$_{int}$ and **6**$_{int}$ merely displayed high-field signals ranging from δ_B −1.13 to −16.12, with the bridging boron signal overlapping with that of the carborane clusters. Therefore, unlike the adduct **LA$_1$**·Et$_3$SiH and **LA$_3$**·Et$_3$SiH that undergo fast equilibrium in solution, the formation of **5**$_{int}$ and **6**$_{int}$ by 1,2-addition of Si–H bond should be irreversible in solution, thus resulting in the purely 4-coordinate bridging boron centers. The single crystal structures of **5**$_{int}$ and **6**$_{int}$ (Figure 4) revealed a
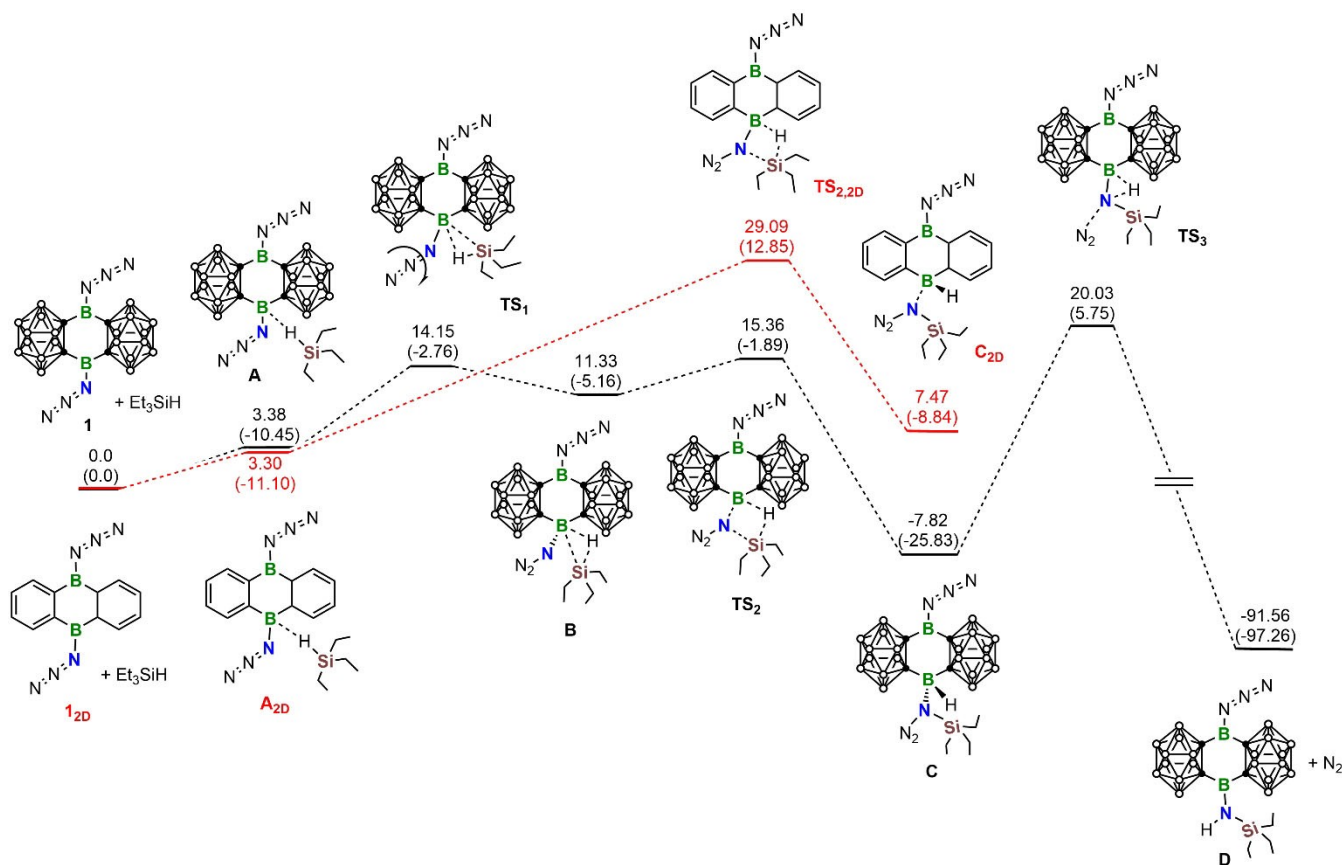
Angew. Chem. Int. Ed. **2022**, *61*, e202205506 (4 of 8)

© 2022 The Authors. Angewandte Chemie International Edition published by Wiley-VCH GmbH

Figure 6. Energy profiles calculated for the reaction from **1** + HSiEt₃ via **A** to **D** + N₂ and from **1₂ᴅ** + HSiEt₃ to **C₂ᴅ**. The relative Gibbs free energies (calculated at 298 k) and electronic energies (in parentheses) are given in kcal mol⁻¹ (in scale).
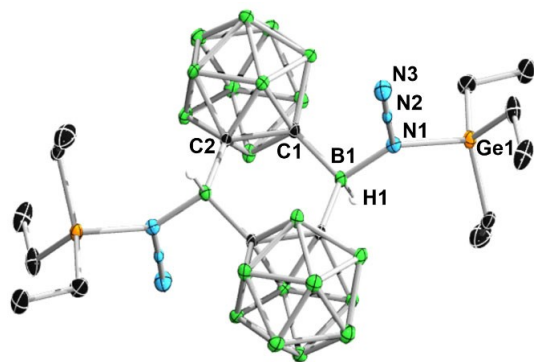

Figure 7. Single crystal structure of **7**. Hydrogen atoms, except for those bound to 4-ccordinate boron, have been omitted for clarity. Thermal ellipsoids are drawn at 50% probability level. Selected bond lengths [Å] and angles [°]: B1–C1 1.637(4), C1–C2 1.688, B1–H1 1.00, B1–N1 1.615(3), N1–N2 1.254(3), N2–N3 1.124(3), N1–Ge1 1.988(2), Ge1–H1 3.146, H1–B1–N1 106.7, B1–N1–Ge1 126.21(15), N1–N2–N3 178.3(2).

significantly longer Si–H distances of 3.072 Å (**5ᵢₙₜ**) and 3.039 Å (**6ᵢₙₜ**) than the H1–Si1 (1.600(16) Å) and H2–Si1 (2.62 Å) distances in **LA₃**·Et₃SiH (Figure 5), suggesting the complete cleavage of the silane Si–H bond. This was further confirmed by the absence of Si–H stretching vibration in the

IR spectrum (Figure S37, S38). On this account, **5ᵢₙₜ** and **6ᵢₙₜ** can also be regarded as the azide-borane adducts (R₃SiN₃)₂.-(C₂B₁₀H₁₀)₂(BH)₂. In fact, the overall geometry of **5ᵢₙₜ** and **6ᵢₙₜ** resemble that of the TMSN₃·B(C₆F₅)₃ adducts,[19] featuring the elongated Si–Nα and B–Nα bonds (**5ᵢₙₜ** Si1–N1 1.856(1) Å, B1–N1 1.626(2) Å; **6ᵢₙₜ** Si1–N1 1.858(3) Å, B1–N1 1.623(4) Å; typical Si–N 1.74 Å, B–N 1.49 Å).[20]

To proof that **5ᵢₙₜ** and **6ᵢₙₜ** are indeed the intermediates for the formation of **5** and **6**, the isolated **5ᵢₙₜ** and **6ᵢₙₜ** were dissolved in C₆D₆ and monitored by multinuclear NMR spectroscopy, respectively. Compound **5ᵢₙₜ** readily released one equivalent of N₂ gas in solution at ambient temperature (ca. 25°C), which was followed by hydride migration from B to N, affording the silyl amino borane **5** (Scheme 3). Nevertheless, the complete conversion required ca. 5 days in C₆D₆ (Figure S39–S44). It should be noticed as well, that **5ᵢₙₜ** was temperature sensitive. At a slightly elevated temperature (38°C), a complete solid-state conversion of **5ᵢₙₜ** to **5** was observed within 3 days. Compound **6ᵢₙₜ** was kinetically more inert than **5ᵢₙₜ** due to the bulk of substituents. A complete conversion at ambient temperature in C₆D₆ required above 7 days (Figure S45, 46). Hence, the successful isolation of **5ᵢₙₜ** and **6ᵢₙₜ** has provided direct evidence for another possible mechanism of formal 1,1-addition reaction on borylnitrene,[1a] and demonstrated an azido borane-based cooperative two-site approach to the Si–H activation.
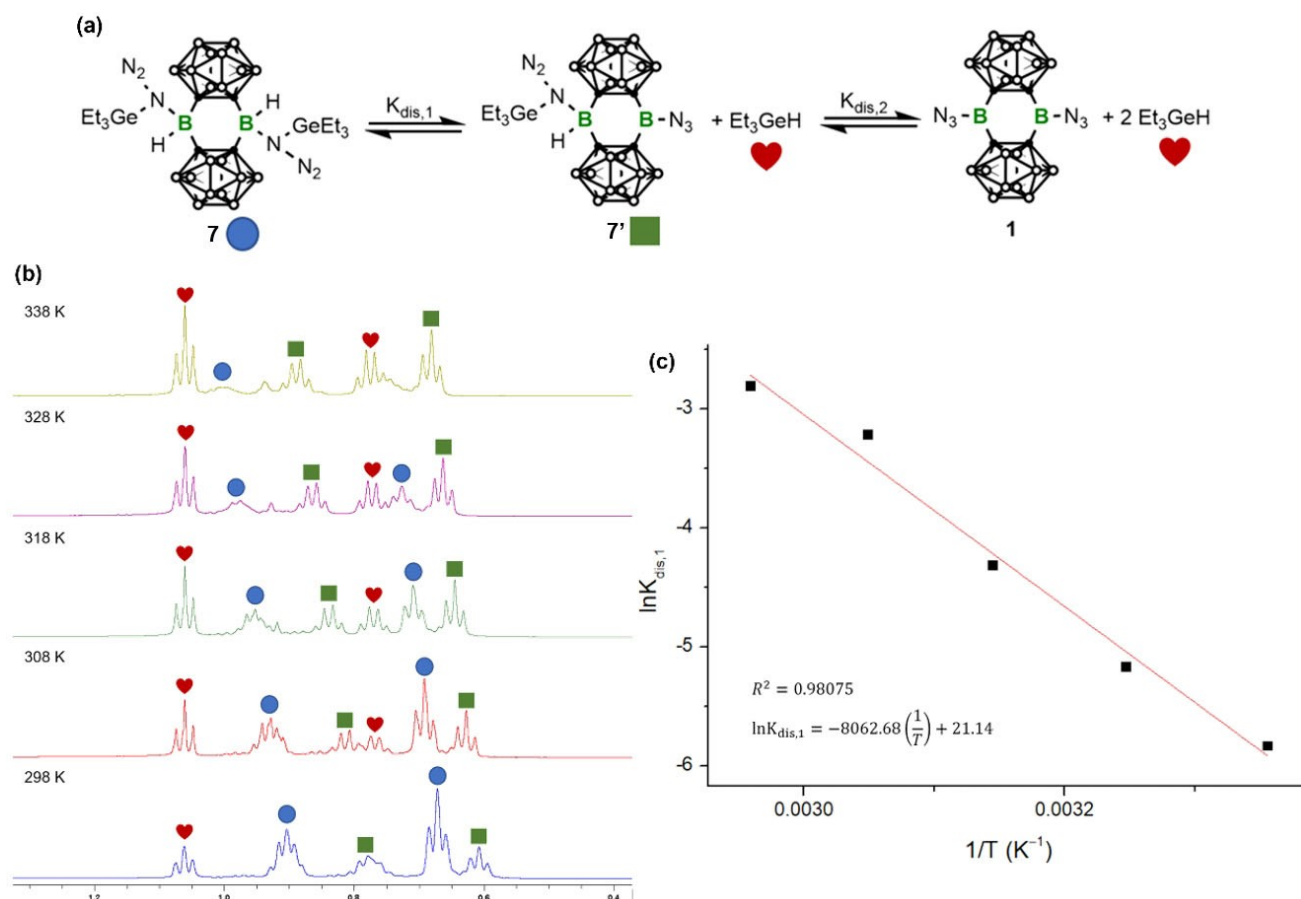
Figure 8. a) Dissociation equilibrium of **7** in solution. b) ^{1}H-NMR spectrum (0.4–1.2 ppm) of **7** at various temperatures. c) Van't Hoff analysis of the equilibrium, which yields thermodynamic parameters $\Delta H° = 16.0$ kcal mol^{-1} and $\Delta S° = 42.1 \times 10^{-3}$ kcal mol^{-1} K^{-1} for $K_{dis,1}$.

DFT calculations were performed to provide further insight into the reaction pathway. All intermediates and transition states were optimized at ωB97XD/6-311g** level of theory (Figure 6). According to the computational results, **1** and HSiEt$_3$ should firstly interact to form the η^1-adduct **A**,[18a] which will be transformed to the η^2-adduct **B**,[10,18b] upon rotation of the azido group (**TS$_1$**). In stark contrast to **LA3**·Et$_3$SiH, the N$_\alpha$ of the azido group triggers the Et$_3$Si-migration (**TS$_2$**), leading to a complete Si–H cleavage. After that, hydride migration accompanied with one equimolar N$_2$ releasing (**TS$_3$**) give the final product **D**. The spontaneity of the migration process is corroborated by the negative ΔG value of -19.1 kcal mol^{-1} for the conversion from **B** to **C**. Considerable barrier (27.8 kcal mol^{-1}) between **C** and **D** allows the isolation of **5$_{int}$** at low temperature. It is worth noting that despite of some slight variations of the energies of the key transformation barriers (Table S12), the reaction pathway which involves both active boron sites led to a similar energy profile as shown in Figure 6. Furthermore, to proof that the Lewis superacidity of **1** is essential for the Si–H cleavage, the same reaction pathway was calculated at the same level of theory with the 2D analogue **1$_{2D}$**, indicating that the Si–H activation barrier of **A$_{2D}$** is 13.7 kcal mol^{-1} higher than **1** and gave a thermodynamic unstable product **C$_{2D}$** which is endergonic by 7.5 kcal mol^{-1} with respect to **1$_{2D}$**.

Thus, the computational results confirmed, to a certain extent, the uniqueness of **1** as a Lewis superacidic azido borane in the cooperative Si–H activation.

To verify the capability of **1** in cooperative Ge–H activation, **1** was reacted with excessive amount of Et$_3$GeH in toluene at 60 °C (Scheme 4). The reaction was monitored by ^{11}B-NMR spectroscopy, which displayed the consumption of **1** and new high-field signals above 5 ppm after 30 mins, excluding the formation of the Ge analogue of **4–6**, $(C_2B_{10}H_2)_2B_2(NH)_2(GeEt_3)_2$. Single crystals of **7** suitable for X-ray diffraction analysis were obtained upon the storage of the reaction mixture at -30 °C for 5 days. The single crystal structure of **7** (Figure 7) resembles that of **5$_{int}$** and **6$_{int}$**, featuring a great Ge–H separation (3.146 Å), and the elongated B–N$_\alpha$ and Ge–N$_\alpha$ bonds (B1–N1 1.615(3) Å, Ge1–N1 1.988(2) Å; typical B–N 1.49 Å, Ge–N 1.89 Å).[21] Although **7** displayed nearly identical N1–N2 bond length when compared to that of **5$_{int}$** and **6$_{int}$** (**7** 1.254(3) Å, **5$_{int}$** 1.268(2) Å, **6$_{int}$** 1.267(4) Å), the calculated energy barrier for the denitrogenation of **7** was 31.3 kcal mol^{-1} (Figure S58), being 3.5 kcal mol^{-1} higher than that of **5$_{int}$** (Figure 6).

In stark contrast to **5$_{int}$** and **6$_{int}$**, a two-step dissociation equilibrium of **7**, which involves **7**, **7′**, **1** and Et$_3$GeH (Figure 8a) existed in solution and was confirmed by VT NMR spectroscopy (Figure 8b: ^{1}H; S51: ^{11}B; S52: ^{13}C).

The ^{1}H-NMR spectrum of **7** displayed five signals ranging from 0.4 to 1.2 ppm at 298 K, which could be assigned to three sets of GeCH$_2$CH$_3$ (Figure 8b, red for Et$_3$GeH; blue for **7**; green for **7**′). The NMR spectra indicated that the equilibrium will be shifted towards the adducts upon a decrease in temperature (Figure 8b, S51–S52), or upon an increase in the concentration of **7** (Figure S53), or upon the addition of extra Et$_3$GeH (Figure S54). The quantitative integration of the signals allowed for the determination of $K_{dis,1}$ for each temperature, which were utilized for the Van't Hoff analysis (Figure 8c), whereupon the thermodynamic parameters for the first-step dissociation were estimated to be $\Delta H° = 16.0\ \mathrm{kcal\,mol^{-1}}$ and $\Delta S° = 42.1 \times 10^{-3}\ \mathrm{kcal\,mol^{-1}\,K^{-1}}$.[22] This corresponds to the Gibbs free energy of 3.5 kcal mol^{-1} at 297 K, which was in excellent agreement with our calculated Gibbs free energy in the gas phase (3.4 kcal mol^{-1}). Moreover, the lower dissociation energy barrier of **7** compared to that of **5$_{int}$** (**7** 19.3 kcal mol^{-1}, **5$_{int}$** 23.2 kcal mol^{-1}) (Figure S58) could explain the remarkable difference in reversibility between the cooperative Si–H and Ge–H activation.

Conclusion

In summary, this work presents a rare example of azido boranes, where both stability and Lewis superacidity were achieved. The Lewis superacidity of **1** was confirmed by the Gutmann-Beckett method and FIA, HIA calculations. Apart from the classical acid-base and Staudinger reactions, the coexistence of the Lewis superacidic boron and an adjacent Lewis basic nitrogen in **1** enabled an azido borane-based cooperative two-site approach to the E–H activation (E = B, Si, Ge). The B–H activation directly led to the 1,1-addition product. The Si–H activation proceeded stepwise via 1,2-addition, denitrogenation and H-migration, overall being equivalent to the 1,1-addition. The Ge–H activation, whilst reversible, stayed at the 1,2-addition step. The isolation of the intermediates **5$_{int}$** and **6$_{int}$** delivered another possible mechanism of the formal 1,1-addition reaction on borylnitrene. Moreover, computational studies indicated that the same reaction of triethylsilane with the 2D 9,10-diazido-DBA is unfavorable, suggesting the uniqueness of **1** as a Lewis superacidic azido borane in the cooperative Si–H activation. Further in-depth studies of this molecular system, as well as the potential application in catalysis are currently underway.

Acknowledgements

Conflict of Interest

The authors declare no conflict of interest.

Data Availability Statement

The data that support the findings of this study are available in the Supporting Information of this article.

[1] a) M. Filthaus, L. Schwertmann, P. Neuhaus, R. W. Seidel, I. M. Oppel, H. F. Bettinger, *Organometallics* **2012**, *31*, 3894–3903; b) R. L. Melen, D. W. Stephan, *Dalton Trans.* **2013**, *42*, 4795–4798; c) E. Merling, V. Lamm, S. J. Geib, E. Lacôte, D. P. Curran, *Org. Lett.* **2012**, *14*, 2690–2693; d) M. Müller, C. Maichle-Mossmer, H. F. Bettinger, *J. Org. Chem.* **2014**, *79*, 5478–5483; e) H. Braunschweig, M. A. Celik, F. Hupp, I. Krummenacher, L. Mailänder, *Angew. Chem. Int. Ed.* **2015**, *54*, 6347–6351; *Angew. Chem.* **2015**, *127*, 6445–6449; f) H. U. Meier, P. Paetzold, E. Schröder, *Chem. Ber.* **1984**, *117*, 1954–1964; g) M. Müller, C. Maichle-Mössmer, H. F. Bettinger, *Angew. Chem. Int. Ed.* **2014**, *53*, 9380–9383; *Angew. Chem.* **2014**, *126*, 9534–9537; h) A. K. Swarnakar, C. Hering-Junghans, M. J. Ferguson, R. McDonald, E. Rivard, *Chem. Sci.* **2017**, *8*, 2337–2343; i) W. Fraenk, T. Habereder, A. Hammerl, T. M. Klapötke, B. Krumm, P. Mayer, H. Nöth, M. Warchhold, *Inorg. Chem.* **2001**, *40*, 1334–1340; j) W. Fraenk, T. Habereder, T. M. Klapötke, H. Nöth, K. Polborn, *J. Chem. Soc. Dalton Trans.* **1999**, 4283–4286; k) E. v. Steuber, G. Elter, M. Noltemeyer, H.-G. Schmidt, A. Meller, *Organometallics* **2000**, *19*, 5083–5091; l) A. K. Swarnakar, C. Hering-Junghans, K. Nagata, M. J. Fgewerguson, R. McDonald, N. Tokitoh, E. Rivard, *Angew. Chem. Int. Ed.* **2015**, *54*, 10666–10669; *Angew. Chem.* **2015**, *127*, 10812–10816; m) T. Thiess, G. Bélanger-Chabot, F. Fantuzzi, M. Michel, M. Ernst, B. Engels, H. Braunschweig, *Angew. Chem. Int. Ed.* **2020**, *59*, 15480–15486; *Angew. Chem.* **2020**, *132*, 15608–15614; n) S. Biswas, I. M. Oppel, H. F. Bettinger, *Inorg. Chem.* **2010**, *49*, 4499–4506; o) W. Fraenk, T. M. Klapötke, *J. Fluorine Chem.* **2001**, *111*, 45–47; p) W. Fraenk, T. M. Klapötke, B. Krumm, P. Mayer, *Chem. Commun.* **2000**, 667–668; q) W. Fraenk, T. M. Klapötke, B. Krumm, P. Mayer, H. Nöth, H. Piotrowski, M. Suter, *J. Fluorine Chem.* **2001**, *112*, 73–81; r) W. Fraenk, T. M. Klapötke, B. Krumm, H. Nöth, M. Suter, M. Warchhold, *J. Chem. Soc. Dalton Trans.* **2000**, 4635–4638; s) U. Müller, *Z. Anorg. Allg. Chem.* **1971**, *382*, 110–122; t) P. I. Paetzold, *Z. Anorg. Allg. Chem.* **1963**, *326*, 47–52; u) P. I. Paetzold, M. Gayoso, K. Dehnicke, *Chem. Ber.* **1965**, *98*, 1173–1180; v) R. L. Melen, A. J. Lough, D. W. Stephan, *Dalton Trans.* **2013**, *42*, 8674–8683.

[2] F. D. Lindl, F. Fantuzzi, L. Mailänder, C. Hörl, G. Bélanger-Chabot, H. Braunschweig, *Chem. Commun.* **2022**, *58*, 4735–4738.

[3] a) P. Müller, H. Pritzkow, W. Siebert, *J. Organomet. Chem.* **1996**, *524*, 41–47; b) H. Schulz, H. Pritzkow, W. Siebert, *Chem. Ber.* **1991**, *124*, 2203–2207; c) J. W. Taylor, W. H. Harman, *Chem. Commun.* **2020**, *56*, 13804–13807; d) J. W. Taylor, W. H.

Harman, *Chem. Commun.* **2020**, *56*, 4480–4483; e) J. W. Taylor, A. McSkimming, M. E. Moret, W. H. Harman, *Angew. Chem. Int. Ed.* **2017**, *56*, 10413–10417; *Angew. Chem.* **2017**, *129*, 10549–10553; f) J. W. Taylor, A. McSkimming, M. E. Moret, W. H. Harman, *Inorg. Chem.* **2018**, *57*, 15406–15413.

[4] a) A. Lorbach, M. Bolte, H. Li, H. W. Lerner, M. C. Holthausen, F. Jakle, M. Wagner, *Angew. Chem. Int. Ed.* **2009**, *48*, 4584–4588; *Angew. Chem.* **2009**, *121*, 4654–4658; b) M. V. Metz, D. J. Schwartz, C. L. Stern, T. J. Marks, P. N. Nickias, *Organometallics* **2002**, *21*, 4159–4168; c) M. V. Metz, D. J. Schwartz, C. L. Stern, P. N. Nickias, T. J. Marks, *Angew. Chem. Int. Ed.* **2000**, *39*, 1312–1316; *Angew. Chem.* **2000**, *112*, 1368–1372; d) V. C. Williams, C. Dai, Z. Li, S. Collins, W. E. Piers, W. Clegg, M. R. J. Elsegood, T. B. Marder, *Angew. Chem. Int. Ed.* **1999**, *38*, 3695–3698; *Angew. Chem.* **1999**, *111*, 3922–3926.

[5] a) S. Brend'amour, J. Gilmer, M. Bolte, H. W. Lerner, M. Wagner, *Chem. Eur. J.* **2018**, *24*, 16910–16918; b) C. M. Hsieh, T. L. Wu, J. Jayakumar, Y. C. Wang, C. L. Ko, W. Y. Hung, T. C. Lin, H. H. Wu, K. H. Lin, C. H. Lin, S. Hsieh, C. H. Cheng, *ACS Appl. Mater. Interfaces* **2020**, *12*, 23199–23206; c) A. Kumar, H. Y. Shin, T. Lee, J. Jung, B. J. Jung, M. H. Lee, *Chem. Eur. J.* **2020**, *26*, 16793–16801; d) C. Reus, S. Weidlich, M. Bolte, H. W. Lerner, M. Wagner, *J. Am. Chem. Soc.* **2013**, *135*, 12892–12907.

[6] E. von Grotthuss, S. E. Prey, M. Bolte, H. W. Lerner, M. Wagner, *J. Am. Chem. Soc.* **2019**, *141*, 6082–6091.

[7] a) M. Dietz, M. Arrowsmith, A. Gärtner, K. Radacki, R. Bertermann, H. Braunschweig, *Chem. Commun.* **2021**, *57*, 13526–13529; b) A. Lorbach, M. Bolte, H.-W. Lerner, M. Wagner, *Organometallics* **2010**, *29*, 5762–5765; c) J. W. Taylor, A. McSkimming, C. F. Guzman, W. H. Harman, *J. Am. Chem. Soc.* **2017**, *139*, 11032–11035; d) E. von Grotthuss, M. Diefenbach, M. Bolte, H. W. Lerner, M. C. Holthausen, M. Wagner, *Angew. Chem. Int. Ed.* **2016**, *55*, 14067–14071; *Angew. Chem.* **2016**, *128*, 14273–14277; e) E. von Grotthuss, S. E. Prey, M. Bolte, H. W. Lerner, M. Wagner, *Angew. Chem. Int. Ed.* **2018**, *57*, 16491–16495; *Angew. Chem.* **2018**, *130*, 16729–16733; f) S. Xu, L. A. Essex, J. Q. Nguyen, P. Farias, J. W. Ziller, W. H. Harman, W. J. Evans, *Dalton Trans.* **2021**, *50*, 15000–15002; g) S. E. Prey, M. Wagner, *Adv. Synth. Catal.* **2021**, *363*, 2290–2309.

[8] Z. Zhou, A. Wakamiya, T. Kushida, S. Yamaguchi, *J. Am. Chem. Soc.* **2012**, *134*, 4529–4532.

[9] H. Zhang, J. Wang, W. Yang, L. Xiang, W. Sun, W. Ming, Y. Li, Z. Lin, Q. Ye, *J. Am. Chem. Soc.* **2020**, *142*, 17243–17249.

[10] C. Zhang, J. Wang, W. Su, Z. Lin, Q. Ye, *J. Am. Chem. Soc.* **2021**, *143*, 8552–8558.

[11] a) V. I. Bregadze, *Chem. Rev.* **1992**, *92*, 209–223; b) M. Scholz, E. Hey-Hawkins, *Chem. Rev.* **2011**, *111*, 7035–7062; c) A. M. Spokoyny, C. W. Machan, D. J. Clingerman, M. S. Rosen, M. J. Wiester, R. D. Kennedy, C. L. Stern, A. A. Sarjeant, C. A. Mirkin, *Nat. Chem.* **2011**, *3*, 590–596.

[12] a) R. Cheng, J. Zhang, J. Zhang, Z. Qiu, Z. Xie, *Angew. Chem. Int. Ed.* **2016**, *55*, 1751–1754; *Angew. Chem.* **2016**, *128*, 1783–1786; b) L. Deng, H. S. Chan, Z. Xie, *J. Am. Chem. Soc.* **2005**, *127*, 13774–13775; c) B. J. Eleazer, M. D. Smith, D. V. Peryshkov, *Tetrahedron* **2019**, *75*, 1471–1474; d) B. J. Eleazer, M. D. Smith, A. A. Popov, D. V. Peryshkov, *Chem. Sci.* **2018**, *9*, 2601–2608; e) S. P. Fisher, S. G. McArthur, V. Tej, S. E. Lee, A. L. Chan, I. Banda, A. Gregory, K. Berkley, C. Tsay, A. L. Rheingold, G. Guisado-Barrios, V. Lavallo, *J. Am. Chem. Soc.* **2020**, *142*, 251–256; f) H. A. Mills, J. L. Martin, A. L. Rheingold, A. M. Spokoyny, *J. Am. Chem. Soc.* **2020**, *142*, 4586–4591; g) Z. Qiu, S. R. Wang, Z. Xie, *Angew. Chem. Int. Ed.* **2010**, *49*, 4649–4652; *Angew. Chem.* **2010**, *122*, 4753–4756; h) S. Ren, Z. Qiu, Z. Xie, *Organometallics* **2012**, *31*, 4435–4441; i) S. Ren, Z. Qiu, Z. Xie, *Organometallics* **2013**, *32*, 4292–4300; j) H. Wang, J. Zhang, H. K. Lee, Z. Xie, *J. Am. Chem. Soc.* **2018**, *140*, 3888–3891; k) S. R. Wang, Z. Qiu, Z. Xie, *J. Am. Chem. Soc.* **2010**, *132*, 9988–9989; l) S. Yao, A. Kostenko, Y. Xiong, A. Ruzicka, M. Driess, *J. Am. Chem. Soc.* **2020**, *142*, 12608–12612; m) S. Yruegas, J. C. Axtell, K. O. Kirlikovali, A. M. Spokoyny, C. D. Martin, *Chem. Commun.* **2019**, *55*, 2892–2895; n) D. Zhao, Z. Xie, *Coord. Chem. Rev.* **2016**, *314*, 14–33; o) L. A. Boyd, W. Clegg, R. C. Copley, M. G. Davidson, M. A. Fox, T. G. Hibbert, J. A. Howard, A. Mackinnon, R. J. Peace, K. Wade, *Dalton Trans.* **2004**, 2786–2799; p) M. Joost, L. Estévez, K. Miqueu, A. Amgoune, D. Bourissou, *Angew. Chem. Int. Ed.* **2015**, *54*, 5236–5240; *Angew. Chem.* **2015**, *127*, 5325–5329; q) J. M. Oliva, N. L. Allan, P. V. Schleyer, C. Viñas, F. Teixidor, *J. Am. Chem. Soc.* **2005**, *127*, 13538–13547; r) H. Wang, L. Wu, Z. Lin, Z. Xie, *J. Am. Chem. Soc.* **2017**, *139*, 13680–13683; s) H. Wang, J. Zhang, Z. Lin, Z. Xie, *Chem. Commun.* **2015**, *51*, 16817–16820; t) H. Wang, J. Zhang, Z. Lin, Z. Xie, *Organometallics* **2016**, *35*, 2579–2582; u) H. Wang, J. Zhang, J. Yang, Z. Xie, *Angew. Chem. Int. Ed.* **2021**, *60*, 19008–19012; *Angew. Chem.* **2021**, *133*, 19156–19160; v) Y. P. Zhou, S. Raoufmoghaddam, T. Szilvási, M. Driess, *Angew. Chem. Int. Ed.* **2016**, *55*, 12868–12872; *Angew. Chem.* **2016**, *128*, 13060–13064.

[13] a) M. A. Beckett, G. C. Strickland, J. R. Holland, K. Sukumar Varma, *Polymer* **1996**, *37*, 4629–4631; b) U. Mayer, V. Gutmann, W. Gerger, *Monatsh. Chem.* **1975**, *106*, 1235–1257.

[14] a) H. Böhrer, N. Trapp, D. Himmel, M. Schleep, I. Krossing, *Dalton Trans.* **2015**, *44*, 7489–7499; b) L. Greb, *Chem. Eur. J.* **2018**, *24*, 17881–17896; c) L. O. Müller, D. Himmel, J. Stauffer, G. Steinfeld, J. Slattery, G. Santiso-Quiñones, V. Brecht, I. Krossing, *Angew. Chem. Int. Ed.* **2008**, *47*, 7659–7663; *Angew. Chem.* **2008**, *120*, 7772–7776.

[15] a) M. O'Keeffe, *J. Am. Chem. Soc.* **1986**, *108*, 4341–4343; b) C. R. Wade, A. E. Broomsgrove, S. Aldridge, F. P. Gabbai, *Chem. Rev.* **2010**, *110*, 3958–3984.

[16] K. F. Purcell, R. S. Drago, *J. Am. Chem. Soc.* **1966**, *88*, 919–924.

[17] a) P. I. Paetzold, P. P. Habereder, G. Maier, M. Sandner, *Fortschr. Chem. Forsch.* **1967**, *8*, 437–469; b) A. Stute, L. Heletta, R. Fröhlich, C. G. Daniliuc, G. Kehr, G. Erker, *Chem. Commun.* **2012**, *48*, 11739–11741.

[18] a) A. Y. Houghton, J. Hurmalainen, A. Mansikkamäki, W. E. Piers, H. M. Tuononen, *Nat. Chem.* **2014**, *6*, 983–988; b) Y. Liu, B. Su, W. Dong, Z. H. Li, H. Wang, *J. Am. Chem. Soc.* **2019**, *141*, 8358–8363.

[19] K. Bläsing, J. Bresien, R. Labbow, D. Michalik, A. Schulz, M. Thomas, A. Villinger, *Angew. Chem. Int. Ed.* **2019**, *58*, 6540–6544; *Angew. Chem.* **2019**, *131*, 6610–6615.

[20] P. Müller, R. Herbst-Irmer, A. L. Spek, T. R. Schneider, M. R. Sawaya, *Crystal Structure Refinement*, *A Crystallographer's Guide to SHELXL*, Oxford University Press, **2006**, pp. 219–220.

[21] M. L. Amadoruge, A. G. DiPasquale, A. L. Rheingold, C. S. Weinert, *J. Organomet. Chem.* **2008**, *693*, 1771–1778.

[22] About NMR dynamic processes. See website: http://chem.ch.huji.ac.il/nmr/techniques/other/dynamic/dynamic.html#ms.

[23] Deposition Numbers 2114968 (for **1**), 2162075 (for **2**), 2162076 (for **3**), 2162077 (for **6**), 2114969 (for **5**$_{int}$), 2162078 (for **6**$_{int}$), 2162079 (for **7**) contain the supplementary crystallographic data for this paper. These data are provided free of charge by the joint Cambridge Crystallographic Data Centre and Fachinformationszentrum Karlsruhe Access Structures service.